Attention in Motion: Using an Oddball Task to Record Brain Activity in Skateboarders

Daniel Robles, Jonathan W. P. Kuziek, Nicole A. Wlasitz, Nathan T. Bartlett, Pete L. Hurd, Kyle E. Mathewson

Department of Psychology
Faculty of Science
University of Alberta

Corresponding Author:

Kyle E. Mathewson, Department of Psychology
(780) 492-2662
P-217 Biological Sciences Building, University of Alberta
Edmonton, Alberta
Canada T6G 2R3
kmathews@ualberta.ca

Number of pages: 33. Total number of figures: 8. Total number of tables: 3

Total number of words in manuscript: 8155. Total number of words in abstract: 178

Keywords: Mobile EEG, ERP, outdoor cognition, portable research

Abstract

Recent advancements in portable technology have opened new avenues in the study of human cognition outside research laboratories. This flexibility in methodology has led to the publication of several Electroencephalography (EEG) studies recording brain responses in real world scenarios such as cycling and walking outside. In the present study, we wanted to test the classic oddball task event related potentials (ERPs) while participants moved around a running track using an electric skateboard. This novel approach allows for the study of attention in motion while virtually removing body movement. Using the auditory oddball paradigm, we were able to measure the P3 and MMN-N2b components elicited by this task. We also found that compared to resting state, alpha power is attenuated in frontal and parietal regions during skateboarding. We also tested for the effect of stance preference in terms of P3 and alpha magnitude and found no differences in for either of these. By replicating the findings of the classic oddball task under such a novel environment this study extends our knowledge of brain function in highly ecologically valid scenarios.

Introduction

For decades the study of human cognition has taken place inside research facilities worldwide. This is largely attributed to the fact that the manipulation and control of the study environment is important in the research process. Electroencephalography (EEG) research has informed our understanding of human attention for decades, yet, what we know from this field generally comes from paradigms that isolate participants in faraday cages to avoid electromagnetic fields and noise compromise data quality (Puce & Hämäläinen, 2017). Over recent years, developments in portable technology and computers have allowed scientists to take studies outside the lab and into the real world. This has been reflected in the growth of mobile EEG studies and studies using ecologically rich environments (Askamp & van Putten, 2014; Kontson et al., 2015; Cruz-Garza et al., 2017; Kuziek et al., 2018).

Mobile EEG research provides an opportunity to further validate our understanding about attention by exploring classic paradigms in real world scenarios. For example, an oddball task in which participants respond to rare stimuli in streams of frequency distractors has classically been used to study attentional allocation. The ERP oddball P3, a positive voltage increase following infrequent tones, (Squires et al., 1975) has been widely reported in EEG studies for decades. This easily elicited ERP is ideal to explore brain responses in more complex real-world environments. There is a long history of using the P3 as a measure of resource allocation in realistic tasks dating back to studies of pilots (Sirevaag et al., 1993), as well as video game training studies showing increase in resources with training (Maclin et al., 2011, Mathewson et al., 2012). Previous studies from our laboratory have successfully recorded ERP components during active physical performance and in real-world scenarios. For example, using an auditory oddball paradigm, Scanlon et al., (2017) reliably recorded the P3 and MMN/N2b components as well as a frontal

alpha peak during stationary cycling. In a follow-up study where participants completed the oddball task cycling outdoors, Scanlon et al., (2019) showed that the P3 and MMN/N2b are present during outside cycling. Additionally, it was found that compared to indoor cycling, there is a reduction in the oddball P3, P2, and alpha peak when cycling outside. This P3 reduction likely can be attributed to an increase in cognitive processing due to being outdoors. Conversely, cycling outside was found to maximize the N1 amplitude for standard and target tones. In the current experiment we are using a real world activity of skateboarding on an indoor 200-meter track to measure ERPs in order to estimate brain resources used by the oddball task similar to this past research on bicycles.

To expand our knowledge about brain functioning outdoors, we employed the mobile methodology used by our lab in a task using skateboarding. By using an e-skateboard we can greatly reduce the amount of body movement in the experiment, which is advantageous over EEG studies with active movement such as walking or cycling. We chose a wirelessly operated skateboard (https://boostedboards.com/ca/) to allow for smooth navigation and to greatly reduce movement artifacts. Following the results from the previous studies in our laboratory, we tested for the allocation of cognitive resources by measuring ERPs during different skateboarding conditions, after first testing whether it is possible to obtain a P3 and MMN/N2b while individuals ride a skateboard. Because studies such as Zink et al., (2016) have also reported a decrease in P3 amplitude in outdoor conditions due to higher cognitive demands, we tested if increased riding difficulty associated with riding in an unpreferred stance would result in a reduction of the P3 response. This could be accomplished by switching the participant riding stance from preferred to non-preferred and looking for resultant changes in the amplitude of ERP components evoked by our secondary oddball task.

In addition to ERPs, oscillatory brain responses have also been used to estimate resource allocation and cognitive engagement in secondary tasks. For example, alpha has been measured in studies of active visuospatial biasing and suppression (Kelly et al., 2009), selective inhibition, and other anticipatory mechanisms (Foxe et al., 1998; Rihs et al., 2007). Alpha power seems to modulate depending on task and place where the task takes place. Studies from our laboratory have shown that during cycling, alpha power decreases outdoors relative to indoors (Scanlon et al., 2019), whereas other studies have shown that relative to a resting baseline, alpha power decreases in walking or riding a stationary bicycle (Storzer et al., 2016). Using the skateboard paradigm, we explored whether alpha power decreases while participants are engaged in a task while minimizing whole body movement using the self-propelling skateboard.

Previous studies looking into the role of alpha in spatial attention have shown that parieto-occipital alpha power increases in the hemisphere contralateral to the side of space containing irrelevant information (Kelly et al., 2006; Ikkai et al., 2016). In the current paradigm, participants ride an e-skateboard around a running track clockwise and counter-clockwise. This allows us to spatially separate the source of incoming distractors based on the direction participants ride. In the clockwise condition (regardless of riding preference) the largest source of distractors (joggers, walkers, and track users) come from the right side of space while in the counter clock condition the source of distraction is always located on the left visual field of the participant. This is because participants were set to only ride in the outermost track during the task.

The current study builds on mobile EEG methodology previously used in our laboratory (Scanlon et al., 2017, Scanlon et al., 2019). Our focus is to use an auditory oddball paradigm in order to explore differences in ERP amplitude in the P3 and MMN components. We tested the

robustness of the oddball P3 effect while participants ride a skateboard on a running track in different conditions (preferred stance clockwise direction, preferred stance counterclockwise direction, non-preferred stance clockwise direction, and non-preferred stance counterclockwise direction). By having participants complete the oddball task in these conditions we can explore the effect of riding stance on P3 amplitude. For the ERP analysis, since dual task processes modulate P3 amplitude (Kramer & Strayer, 1988; Kida et al., 2012), we predict a decrease in P3 amplitude in the non-preferred stance due to increases in riding difficulty while completing the task.

In terms of stance preference and alpha power, we are expecting to measure higher Fz, and Pz alpha power in the non-preferred condition due increases in task demand associated with riding difficulty. Additionally, we are computing the averaged alpha power between the left and right electrodes to further explore whether lateralization changes based on riding stance. In terms of alpha lateralization and riding position, the current paradigm provides an opportunity to explore whether distracting areas in the visual field influence alpha power in between left-right hemisphere. Spatial attention paradigms, such as Kelly et al., (2006) and Sauseng et al., (2005), demonstrated that alpha power increases over areas to be ignored, so we expect to see an increase of alpha power in the parieto-occipital region contralateral to the source of distractors in the clockwise and counterclockwise riding directions. Using this indoor track and mobile EEG paradigm, we expect to reliably measure ERPs using the oddball task while exploring the influence of riding difficulty and distractors in ERP and oscillatory rhythms.

Methods

Participants

A total of 29 individuals from the broader university community completed the study (mean age = 20.96, age range = 18-27). Participants received either an honorarium of $20 or credits towards Research Participation in an undergraduate psychology class. All participants had normal or corrected-to-normal vision and a history free from neurological conditions. Each participant was comfortable with basic skateboarding in both preferred and non-preferred stances. This study was approved by the Internal Research Ethics Board at the University of Alberta (Pro00050069) and participants gave informed consent before completing the study. This study conforms with the World Medical Association Declaration oh Helsinki.

Materials and Procedure

The experiment was completed in the Universiade Pavillion (aka Butterdome) on a 200-meter indoor track at the University of Alberta. Participants first completed two, three-minute, resting-state tasks (either eyes closed or eyes open) to measure a baseline level of spectral activity while they were seated in the bleachers of the track. Participants were instructed to breathe calmly and either keep their eyes closed, or to fixate on a nearby object. Following both baseline tasks, participants were given a basic tutorial on using the Boosted V3 Stealth Electric Board (Palo Alto, California, United States; https://boostedboards.com/ca/) before starting the main skateboard experiment. The Boosted skateboard is a two-motor electric skateboard controlled by a joystick held in the right hand with throttle and clutch controls on the thumb and trigger finger respectively. The joystick was held in their right hand while a response button was held in their left hand. Participants began the task by standing on the skateboard and pressing the response button, starting a 10-second countdown. Participants were expected to be in motion around the Universiade Pavilion track when the countdown finished. To ensure clean data,

participants were instructed to remain as still as possible, blink only when necessary, and keep their gaze directed forward.

Based on the participant's preferred skateboarding stance and the direction the participant travelled around the Pavilion track, four conditions were generated: 'preferred clockwise', 'preferred counter-clockwise', 'non-preferred clockwise', and 'non-preferred counter-clockwise'. Condition order was randomly determined and counter-balanced. In each condition, participants completed an auditory oddball task where two tones were consistently presented through headphones (either a 1000 Hz or 1500 Hz tone). Participants were instructed to press the response button each time the 1500 Hz tone was played (target tone) and to withhold a response following the 1000 Hz tone (standard tone). A delay, randomly selected from a distribution between 1000 and 1500 ms, followed each tone. Response times were collected during this delay period. In all, 20% of trials contained a target tone and 80% contained a standard tone, with 250 trials in each condition. Each condition was approximately six minutes long. Between conditions, the participant returned to the starting position, the computers were reset, and the participant was given a small break.

The tones and response button task were programmed and administered using a Raspberry Pi 2 model B computer (Raspberry Pi Foundation, Cambridge, UK) running version 9 of the Raspbian Stretch operating system and version 2.7.13 of Python. The Raspberry Pi 2 was powered via a micro-USB cable connected to a Microsoft Surface Pro 3 laptop. Audio output was via Sony earbuds connected to the 3.5mm audio connector on the Raspberry Pi 2. Coincident in time with tone onset, 8-bit TTL pulses were sent to the EEG amplifier via a cable connected to the GPIO pins of the Raspberry Pi 2. These trigger markers were used to mark the EEG data for ERP averaging. EEG data was collected from participants using active, wet, low-

impedance electrodes (actiCAP active electrodes kept below 5 kΩ). Inter-electrode impedances were measured at the start of the experiment. The following electrode locations were used, arranged in the typical 10-20 electrode positions (F3, F4, T7, T8, C3, C4, P7, P8, P3, P4, O1, O2, Fz, Cz, Pz). A ground electrode was used, positioned at AFz. Ag/AgCl disk electrodes with SuperVisc electrolyte gel and mild abrasion with a blunted syringe tip were used to lower impedances. EEG data was recorded online referenced to an electrode attached to the left mastoid. Offline, the data were re-referenced to the arithmetically derived average of the left and right mastoid electrodes.

EEG data was recorded with a Brain Products V-Amp 16-channel amplifier (Brain Products GmbH), connected to the same Microsoft Surface Pro 3 laptop powering the Raspberry Pi, running BrainVision Recorder software (Brain Products GmbH, Gilching, Germany)). In addition to the 15 EEG sensors, two reference electrodes, and the ground electrode, vertical and horizontal bipolar EOG was recorded from passive Ag/AgCl easycap disks using Bip2Aux adapters connected to the auxiliary ports of the amplifier. EOG electrodes were affixed vertically above and below the left eye and affixed horizontally 1 cm lateral from the outer canthus of each eye. The participant's skin was cleaned using Nuprep (an exfoliating cleansing gel) (Weaver & Co, Aurora, Colorado USA) before the placement of the electrodes, electrolyte gel was used to lower the impedance of these electrodes to under 5 kΩ in the same manner as previously mentioned. Data were digitized at 1000 Hz with a resolution of 24 bits and hardware filtered online between 0.1 Hz and 30 Hz, with a time constant of 1.5155 s and a notch filter at 60 Hz. All aforementioned equipment was held within 2-pocket backpack worn on by the participant, as shown in Figure 1.

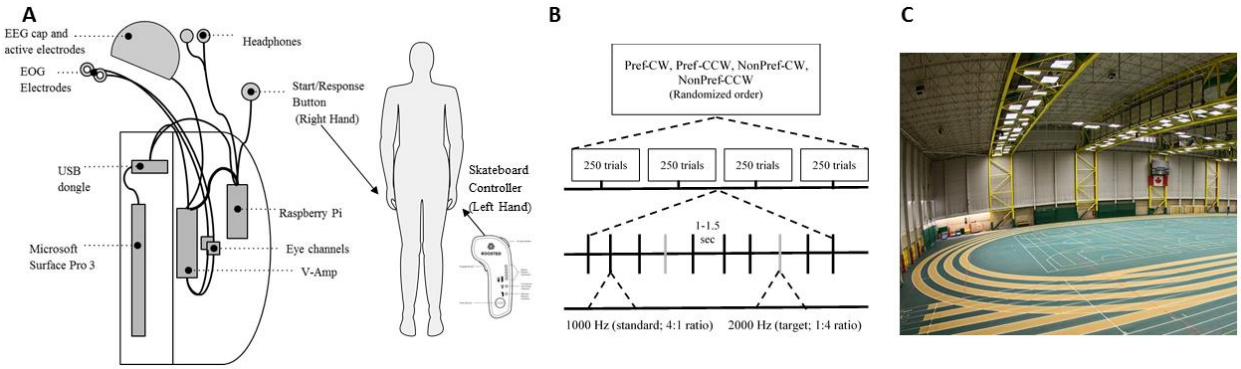

Figure 1. Setup task and Location. A: Backpack setup. B: Task diagram. C: Experiment location

EEG Analysis

Analyses were computed in Matlab R2018a (Mathworks, Natick, Massachusetts, USA) using EEGLAB (Delorme & Makeig, 2004) and custom scripts (https://github.com/kylemath/MathewsonMatlabTools). Statistical analyses were computer on JASP (JASP Team, Amsterdam, Netherlands). The EEG markers were used to construct 1200 ms epochs time locked to the onset of standard and target tones, with the average voltage in the first 200 ms baseline period subtracted from the data for each electrode and trial. To remove artifacts due to amplifier blocking and other non-physiological factors, any trials with a voltage difference from baseline larger than +/- 1000 µV on any channel (including eyes) were removed from further analysis. At this time, a regression-based eye-movement correction procedure was used to estimate and remove the artifact-based variance in the EEG due to blinks as well as horizontal and vertical eye movements (Gratton et al., 1983). After identifying blinks with a template-based approach, this technique computes propagation factors as regression coefficients predicting the vertical and horizontal eye channel data from the signals at each electrode. The eye channel data is then subtracted from each channel, weighted by these propagation factors, removing any variance in the EEG predicted by eye movements. Artifact rejection was again performed except for this second round of artifact rejection removed trials containing a voltage

difference of +/- 500µV. These artifact rejection thresholds were chosen to be relatively lenient to similar to other mobile EEG studies we have done (Scanlon et al., Scanlon et al., 2017, Scanlon et al., 2019, Scanlon et al., 2020) in order to quantify how much noise (electrical, muscle, or otherwise) was present in the ERP data and to ensure an adequate number of trials were available for analysis. Baseline correction was performed again following the second artifact rejection.

ERP analysis

Appropriate time window cut-offs for the MMN/N2-B and P3 waveforms were determined by creating grand-average ERP waveforms, averaged across all participants and conditions, to create a single ERP waveform for electrodes Fz and Pz (Figure 2). These grand-average waveforms were used to avoid biasing the selected time windows towards any one condition. The negative deflection between 195-295 ms for electrode Fz was used for the MMN/N2-B time window while the large positive deflection between 375-525 ms for electrode Pz was used for the P3 time window. Trial-averaged ERPs were derived in each of the four conditions (‘preferred clockwise’, ‘preferred counter-clockwise’, ‘non-preferred clockwise’, and ‘non-preferred counter-clockwise’) and waveforms were compared. A 4-by-2 ANOVA was run to compare tone type (standard and target) across the four conditions, during the MMN/N2-B and P3 time windows at electrodes Fz and Pz respectively. Pairwise comparisons resulting from the ANOVA analysis were also performed. A two-tailed t-test was also performed on the difference waveforms to compare across preference type (preferred and non-preferred) as we expect to find reduction in P3 in the non-preferred condition, for each time window. These waveforms were derived by subtracting the standard ERP waveforms from the target ERP

waveforms for both the preferred and non-preferred conditions, with α set to 0.05 for all analyses.

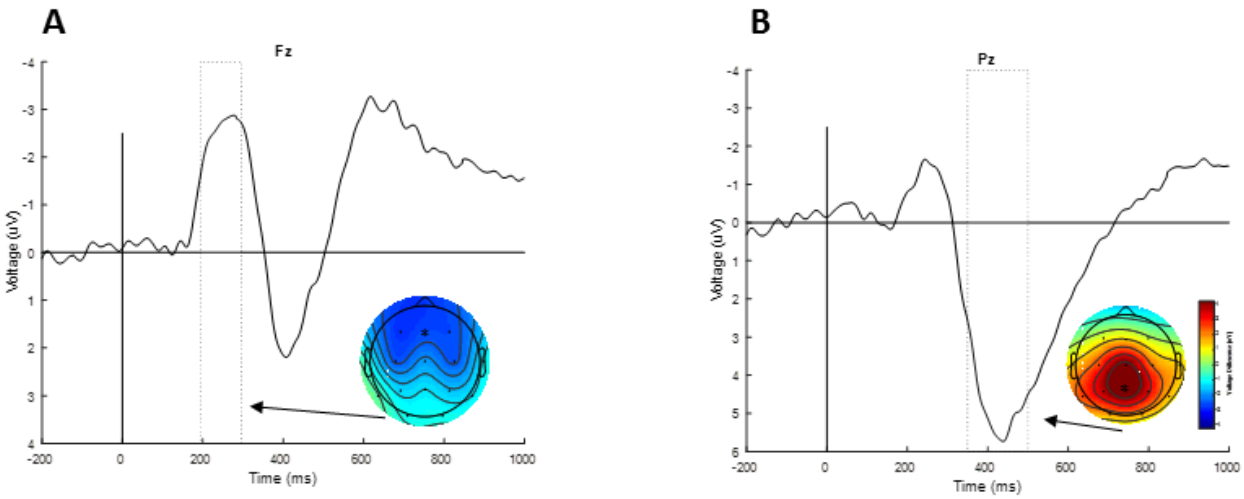

Figure 2. Grand-averaged ERP across conditions used to select time windows for analyses.

Spectral Analysis

Average frequency spectra across the baseline and oddball epochs was also computed using the wavelet routine from the Better Oscillation Method (BOSC; Whitten et al., 2011) with a 12 cycle wavelet transform across a frequency range of 0.1 Hz to 30 Hz, increasing in 0.5 Hz steps. Spectral data was further analyzed using the "Fitting Oscillations & One Over F" (FOOOF) algorithm (Haller et al., 2018) to represent the data as two distinct components; the aperiodic background 1/*f* and periodic oscillations which may contain greater spectral power than the aperiodic component. This analysis was performed using version 0.1.1 of the FOOOF Matlab wrapper with the following settings: peak width limits = [0.5,12]; max number of peaks = Inf; minimum peak amplitude = 0.0; peak threshold = 2.0; background mode = fixed; verbose = true; frequency range = 0.5-30 Hz. The background 1/*f* spectra was then subtracted from the periodic component to better compare changes in spectral power between 0.5 Hz and 30 Hz across our conditions. All spectral analyses were done using this calculated FOOOF spectral data.

For the baseline task spectra were computed for each participant, averaged across the entire three-minute duration of each condition (eyes open and eyes closed), and then combined across participants to generate grand-averaged spectra for each condition. For the oddball task, we generated 3000 ms epochs around the onset of each standard trial (1000 ms pre and 2000 ms post standard onset) for each participant. Spectra were calculated for each epoch, then averaged across time and number of standard trials to generate spectra for each participant. These spectra were then averaged across participants to create grand-average spectra for each condition in the oddball task. Spectra were calculated using electrodes Fz and Pz. Furthermore, in order to evaluate the role of stance preference in hemispheric alpha power, we compared the averaged power of the left and right hemisphere using the following combination of electrodes: left power sources (F3, T7, C3, P3, P7, O1), right power sources (F4, T8, C4, P4, P8, O2). In order to explore the role of left-right visual field distractors in hemispheric alpha, power was computed by combining the following parieto-occipital electrodes: left hemisphere (P7, P3, O1), right hemisphere (P8, P4, O2).

Results

Behavioral Results

Table 1 shows the mean trial count for target and standard tones used for each condition after artifact rejection. The rejected number of trials for targets and standards respectively was similar for all conditions($F(3,112) = 0.84$, $p = 0.48$). Figure 3A shows the mean accuracy in response to standard tones across all four task conditions and by global stance preference (collapsed over direction of travel). Results from a repeated measures one-way ANOVA shows no differences in accuracy across these four conditions, $F(3, 84) = 0.64$, $p = .55$. A one-tail t-test suggests no statistically significant difference between the preferred stance (M = 93.68; SD =

1.18), and non-preferred stance (M= 92.89; SD = 1.46); $t(28) = 0.86$, $p = .19$. Figure 3B shows mean reaction times in milliseconds for all four task conditions and by global stance preference. A one-way ANOVA suggests no significant differences in reaction time between conditions, $F(3, 84) = .085$, $p = .96$. A one-tail t-test computed for difference mean reaction time across global stance shows no significant differences between preferred stance (M = 504.68 ms; SD 7.85) and non-preferred stance (M = 504.82 ms; SD 10.03); $t(28) = -0.01$, $p = .49$).

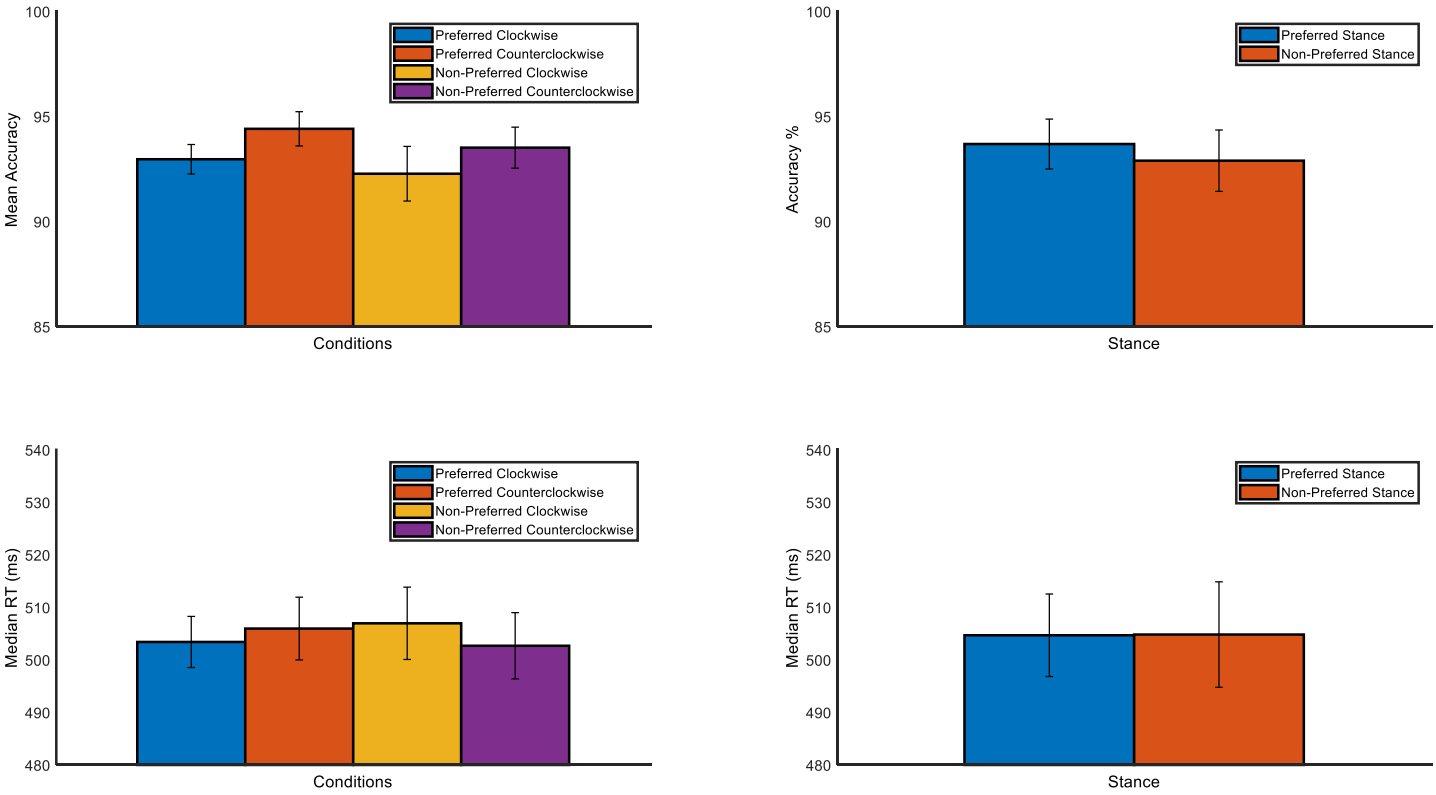

Figure 3. A: Response accuracy for original conditions and by overall preference. B: Reaction time for original conditions and by overall preference.

Condition	Stimulus Type	Mean Trial Count	Standard Deviation	Trial Count Range (Minimum:Maximum)
Preferred Clockwise	Targets	46.90	4.87	29:50
	Standards	185.83	21.61	104:200
Preferred Counter-Clockwise	Targets	47.79	5.06	26:50
	Standards	191.52	17.35	115:200
Non-preferred Clockwise	Targets	47.90	4.47	30:50
	Standards	190.34	17.59	131:200
Non-preferred Counter - Clockwise	Targets	47.76	4.56	29:50
	Standards	189.79	20.75	92:200

Table 1: Trial count information for targets and standards in each condition.

ERP Morphology and Topography

Figure 4A shows the grand average ERPs for target and standard tones at electrode Fz for all study conditions. Standard errors at each time point are depicted by the shaded regions. These plots show that compared to standard tones, there is an increase in negative voltage for the MMN/N2 time window between 195 and 295 ms following target tones. Figure 4C shows the grand average ERP at electrode Pz for all conditions. These grand average ERPs show a clear positive increase in voltage in the P3 window, between 350 and 550 ms following target tone onset. Additionally, topographies were computed for the MMN/N2b and P3 time windows across conditions to show the overall scalp activation distribution for both time windows. Based on the time window chosen for these topographies, one can observe a more anterior distribution for the MMN/N2b time window and a more posterior distribution for the P3 time window. We conducted a 2x4 repeated measures ANOVA in order to understand the relationship between target/standard tones in all four conditions and whether the MMN/N2-B and P3 are influenced by riding condition. For the early time window at electrode Fz, there was a significant main effect

for tone type $F(1,28) = 87.72$, $p < .001$. There was no significant main effect for condition ($F(3,84) = 1.55$, $p = .29$) and no significant interaction of tone and condition ($F(3,84) = 1.42$, $p = .24$).

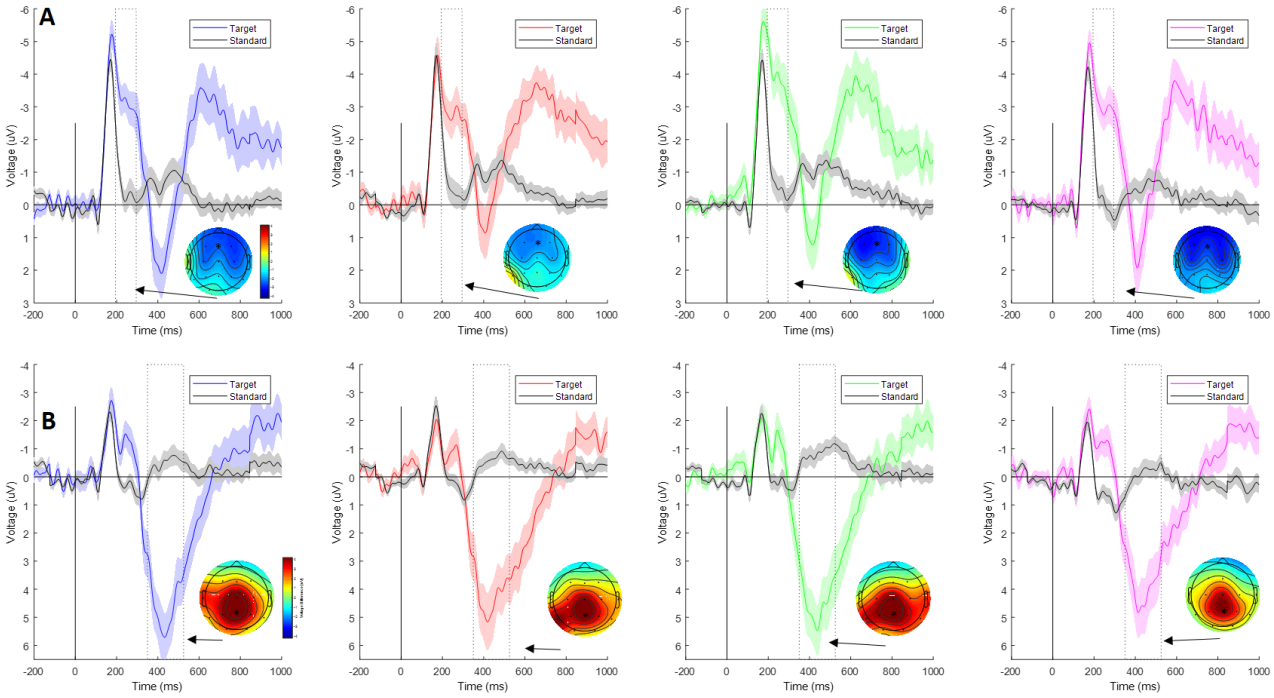

Figure 4: A: ERPs at Electrode Fz. Conditions (left to right): Preferred clockwise, preferred counter clock-wise, non-preferred clockwise, non-preferred counter clockwise. Target tones: colored lines. Standard tones: black lines. Shaded regions represent standard errors. Topographies for MMN/N2 window. B: ERPs at Electrode Pz. and topographies for P3 time windows.

Table 2 shows the significant pairwise comparisons where it can be seen that the target-standard difference at the MMN/N2b window was reliable in all four conditions. For the P3 window at electrode Pz, a repeated measures two-way ANOVA revealed a significant main effect for tone type, $F(1,28) = 50.86$, $p < .001$. There was not a significant main effect for condition type ($F(3,84) = .12$, $p = .94$) and no significant interaction for tone and condition ($F(3,84) = .97$, $p = .41$). Table 2 shows the pairwise comparisons at electrode Pz where, across all conditions, the oddball P3 difference between targets and standards was highly reliable.

Comparison	Electrode/Time Window	Mean Voltages (µV) (Targets : Standards)	*t*(28)	*p*	Confidence Interval
Preferred Clockwise	Fz/MMN-N2b	-3.23:-0.58	-5.98	3.52e-7	-3.48:-1.84
	Pz/P3	4.71:-0.47	5.17	1.03e-7	3.69:6.68
Preferred Counter Clockwise	Fz/MMN-N2b	-2.86:-0.72	-5.64	4.17e-5	-3.04:-1.24
	Pz/P3	4.35:-0.54	4.44	*2.33e-5*	2.91:6.87
Non-preferred Clockwise	Fz/MMN-N2b	-3.96:-0.75	-6.20	1.55e-5	-4.47:-1.95
	Pz/P3	4.59:-0.78	5.81	7.06e-7	3.64:7.11
Non-preferred Counter Clockwise	Fz/MMN-N2b	-3.10:-0.30	5.53	2.39e-6	-3.77:-1.83
	Pz/P3	3.95:-0.05	-4.91	1.39e-4	2.14:5.86

Table 2: Pairwise results comparing target and standard ERP waveforms in each condition.

ERPs and Stance Preference

In order to explore whether riding preference alone influences the P3 and MMN/N2b in the oddball task, we conducted an additional ERP analysis on the grand averaged preferred and non-preferred ERPs for both time windows, collapsed over the direction of travel on the track. It is important to keep in mind that preference was chosen for this analysis because riding in a non-preferred stance increases riding difficulty by requiring participants to devote more resources to their stance/balance while completing the task. Figure 5A shows the grand averaged ERP for target and standard tones in the preferred (left side), and non-preferred stance condition (right side) at electrode Fz. Standard errors for each time point are depicted in the shaded regions. Figure 5B shows the difference-wave ERP for the preferred and non-preferred stance along with difference topographies in the MMN/N2b time window. Such topographies show an overall negative voltage distribution across the scalp for the MMN/N2b time window for the preferred and non-preferred conditions. We conducted a two-tail t-test on the difference wave ERP for the

preferred and non-preferred conditions. Such t-test revealed no significant MMN/N2b differences in stance preference at electrode Fz (Mdiff = 0.60; SD = 2.28; $t(28) = 1.42$, $p = .16$).

Figure 5D shows the grand averaged ERPs for target and standard tones in the preferred stance (left panel) and non-preferred stance (right panel) at electrode Pz. Figure 5E shows the difference-wave ERP by preference Pz with its corresponding difference topographies for the P3 time windows. These topographies show an overall more positive voltage distribution toward Pz, particularly in the preferred stance. We conducted a two-tail t-test on the difference-wave ERP for the preferred and non-preferred stance. The test shows no significant differences in the P3 for stance preference (Mdiff = 0.42; SD = 2.95; $t(28) = 0.63$, $p = .52$).

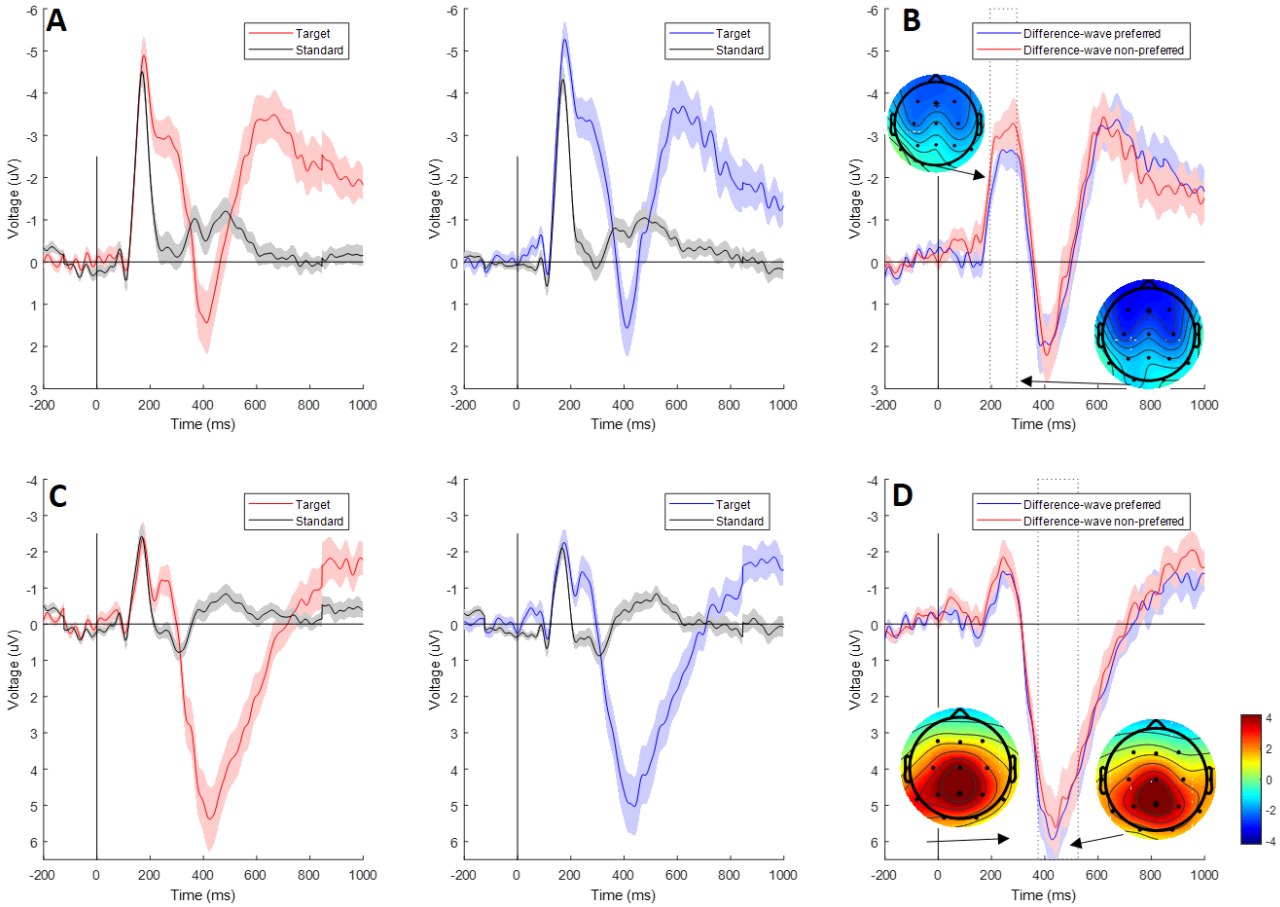

Figure 5. A: ERPs by preference at Fz. Preferred stance (left), non-preferred stance(right). Target tones: colored lines. Standard tones: black lines. Shaded regions represent standard errors.

Difference Topographies for MMN/N2 time window. B: difference-wave ERP by preference C: Preference ERPs at electrode Pz. D: difference-wave ERP by preference. Difference Topographies for P3 time window.

Spectral Results

Figure 6A shows the power spectra plots for all four conditions for frequency range 1-30 Hz at electrode Fz. Resting state baseline spectra for eyes open-close conditions is also depicted. These resting-state power spectra show a predominant peak within the alpha frequency range (8-12 Hz) which is larger during the eyes closed condition. Power topographies for the preferred and non-preferred clockwise conditions (upper region) and preferred and non-preferred counterclockwise conditions (lower region) were generated for the alpha frequency range. Topographies show higher power distribution across central parietal-occipital regions particularly in the non-preferred conditions. Figure 6B shows the power spectra for all conditions and baseline at electrode Pz. This spectra plot shows a clear peak in the alpha frequency in the resting state condition that is more predominant in the eyes closed condition. Relative to the resting state, there is no peak in the alpha frequency in any of the four riding conditions. A one-way ANOVA was conducted in order to assess the differences in alpha peak for all conditions. For electrode Fz, the ANOVA revealed a significant effect for condition type in the alpha range $F(5,156) = 23.74$, $p < .001$.

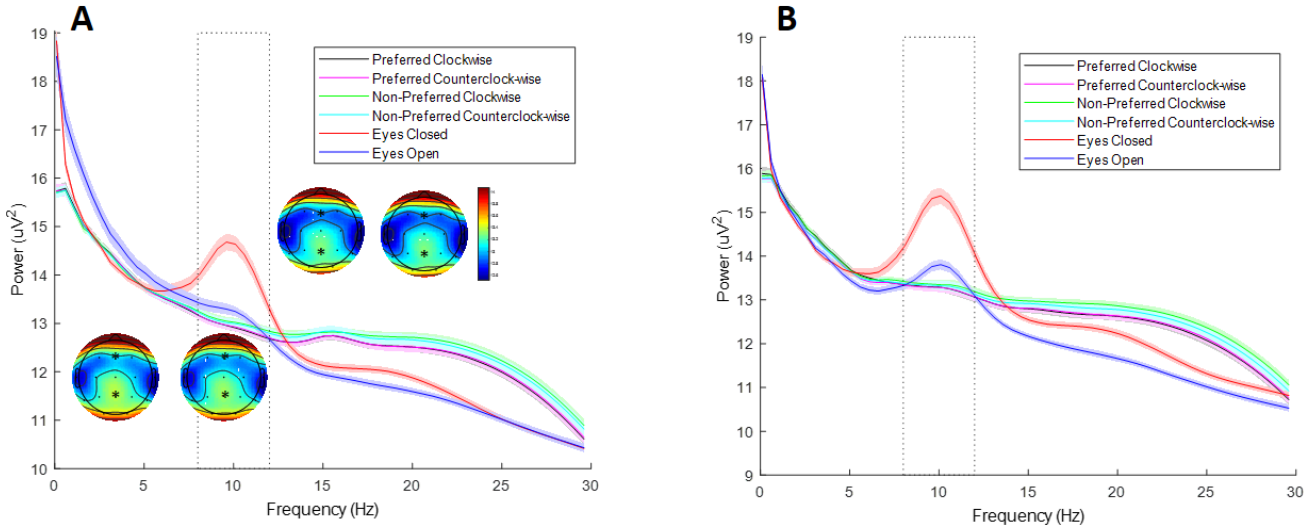

Figure 6. A: Power spectra at electrode Fz for all conditions plus resting state baseline (eyes opened/closed). Shaded regions represent standard errors for all conditions. Power topographies for alpha band range (8-12Hz) for preferred clockwise and counter clockwise conditions (upper region) and non-preferred clockwise and counter clockwise conditions (lower region). B: Power spectra at electrode Pz for all conditions.

Table 3 shows the significant pairwise comparisons. This analysis shows that the resting state/eyes closed condition is significantly different from the rest of conditions. There are no further significant differences between conditions. For electrode Pz, the main effect for condition type in the alpha frequency was significant $F(5,156) = 30.74$, $p < .001$. Table 3 shows the significant pairwise comparisons, and like electrode Fz, the eyes closed condition is significantly different from the rest of the conditions. There were no significant pairwise comparisons between the eyes opened condition and the four riding conditions.

A

Comparison	Electrode	Mean Spectra Difference (μV^2)	*t*(28)	*p*	Confidence Interval
Baseline Eyes Open	Fz	0.43	10.92	<0.001	0.30:0.55
	Pz	0.35	11.34	<0.001	0.25:0.45
Preferred Clockwise	Fz	0.60	11.92	<0.001	0.43:0.76
	Pz	0.74	10.76	<0.001	0.52:0.96
Preferred Counter Clockwise	Fz	0.59	11.14	<0.001	0.42:0.76
	Pz	0.75	10.32	<0.001	0.51:0.98
Non-preferred Clockwise	Fz	0.61	11.55	<0.001	0.44:0.79
	Pz	0.75	11.55	<0.001	0.54:0.96
Non-preferred Counter Clockwise	Fz	0.59	11.30	<0.001	0.42:0.76
	Pz	0.74	11.26	<0.001	0.53:0.95

B

Comparison	Electrode	Mean Spectra Difference (μV^2)	*t*(28)	*p*	Confidence Interval
Baseline Eyes Closed	Fz	0.43	10.92	<0.001	0.30:0.55
	Pz	0.35	11.34	<0.001	0.25:0.45
Preferred Clockwise	Fz	0.17	3.84	6.0e-3	0.03:0.31
	Pz	0.39	5.95	<0.001	0.18:0.60
Preferred Counter Clockwise	Fz	0.16	3.76	6.0e-3	0.02:0.30
	Pz	0.40	6.06	<0.001	0.19:0.62
Non-preferred Clockwise	Fz	-0.19	-4.37	2.0e-3	-0.33:-0.05
	Pz	-0.41	-6.57	<0.001	-0.61:-0.21
Non-preferred Counter Clockwise	Fz	-0.16	-3.96	5.0e-3	-0.29:-0.03
	Pz	-0.39	-6.33	<0.001	-0.59:-0.19

Table 3: Pairwise results comparing A) Baseline Eyes Closed and B) Baseline Eyes Open spectra to each of the other five conditions.

Power Spectra by Preference

We wanted to investigate if riding preference alone could have an effect in alpha power. We computed the grand averaged power in the preferred and non-preferred conditions respectively for an additional analysis. Figure 7A Shows the power spectra distribution for frequency range 0-30 Hz at electrode Fz for the grand averaged preferred and non-preferred conditions. In order to investigate whether alpha spectra changes by riding preference we conducted a one-tail t-test on the power difference between the preferred and non-preferred conditions. Such test revealed no significant differences in spectra for the alpha range between conditions, (Mdiff = -0.004; SD = 0.06; $t(28) = 0.41$, $p = .68$). Figure 7B shows the power spectra at electrode Pz for the grand averaged preferred and non-preferred conditions.

Additionally, no significant differences in alpha power were found at electrode Pz for the preferred and non-preferred conditions (Mdiff = -0.003; SD = 0.10; $t(28) = 0.15$, $p = .88$).

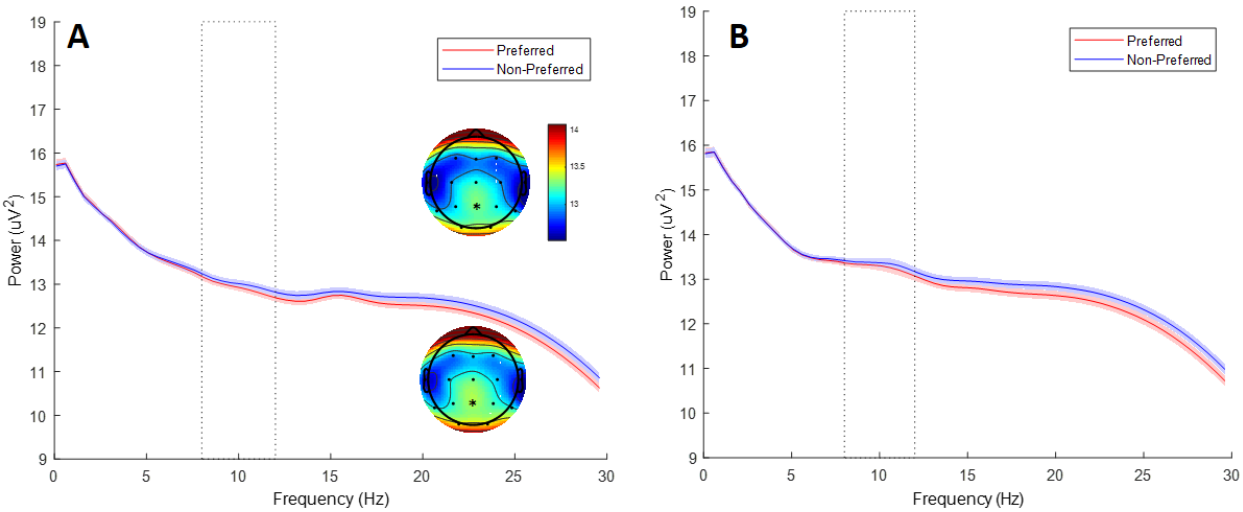

Figure 7. A: Power spectra by stance preference for electrode Fz. Power topographies for preferred (left) and non-preferred (right side) stance for frequency range 8-12Hz. B: Power spectra for preferred and non-preferred stance at electrode Pz.

Left-Right Hemispheric Alpha by Preference and Riding Orientation

In order to address whether hemispheric alpha is influenced by riding preference, we computed the left minus right hemispheric alpha power for the preferred and non-preferred blocks. Figure 8A shows the power spectra for the left and right hemisphere in the preferred stance (left panel) and non-preferred stance (right panel). Figure 8C (below) shows the bar plot of mean power by riding preference. A two tail test revealed no differences in lateralization changes by riding stance $t(28) = .006$, $p = .99$. Additionally, in order to investigate whether peripheral distractors influence alpha lateralization (due to the role of alpha synchronization in suppressing irrelevant areas of the visual field), we compared the left minus right hemisphere difference in alpha band power based on riding orientation (clockwise vs counterclockwise).

Figure 8B shows the left and right parieto-occipital alpha power by riding direction in the clockwise (left side panel) and counterclockwise (right panel) conditions. Figure 8D (below) shows the bar plot of mean power by riding orientation. In order to assess whether lateralization changes by peripheral distractors, we conducted a t-test of the power difference between left-right hemispheres in the clockwise and counterclockwise conditions. Such test revealed no differences in hemispheric alpha power between conditions $t(28) = -0.17$, $p = .86$.

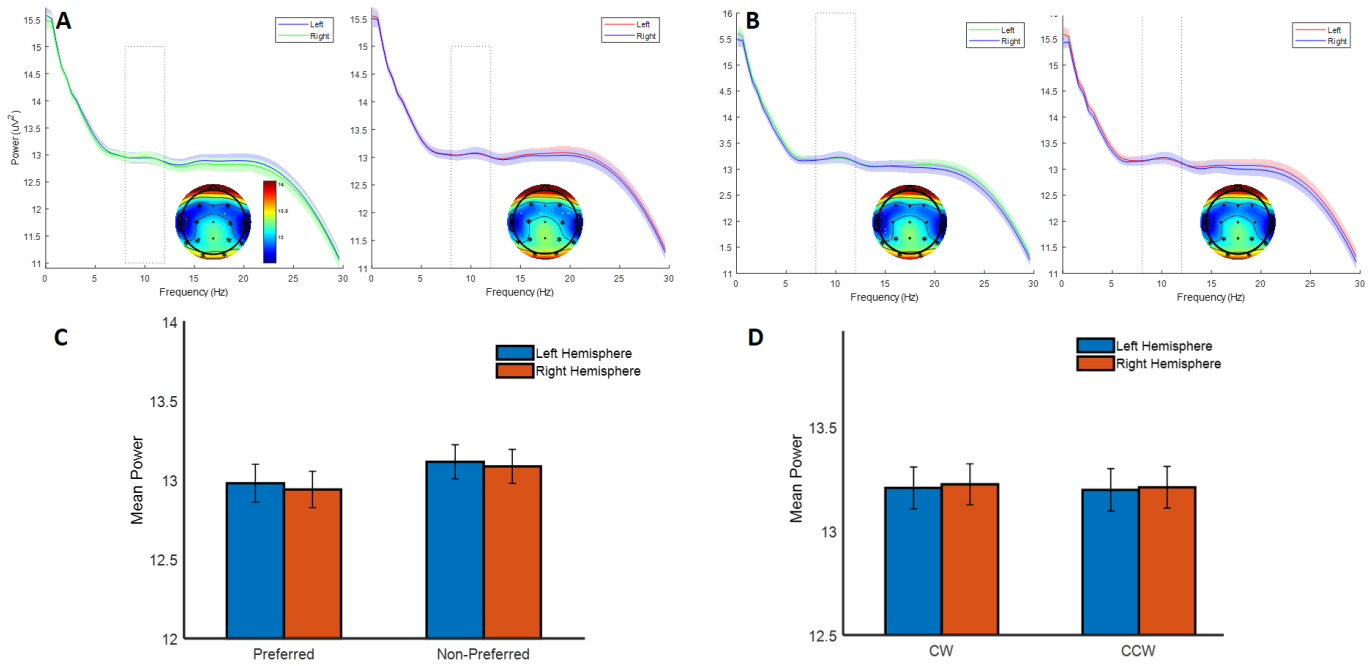

Figure 8. A: Power spectra for left and right hemispheres for preferred (left) and non-preferred stance (right). Power topography for preferred and non-preferred conditions. B: Power spectra for left and right parieto-occipital hemispheres for clockwise direction (left) and counterclockwise direction (right). Power topography for clock and counterclockwise conditions. C: Bar plot of alpha power for left and right hemispheres in the preferred and non-preferred conditions. D: Bar plot of alpha power for left and right parieto-occipital regions for clockwise and counterclockwise conditions.

Discussion

The present study employed a mobile EEG paradigm to successfully record ERP components and oscillatory activity from participants moving on an e-skateboard. Participants responded to an auditory oddball task while riding around a complex real world scenario. To our knowledge, this is the first portable EEG experiment ever published using active skateboarding. We chose to use a skateboarding paradigm for several reasons: We wanted to deploy the mobile EEG methodology previously developed in our laboratory (Kuziek et al, 2017; Scanlon et al, 2017) to a novel scenario as it is important to demonstrate that this mobile EEG methodology can help researchers design and test attentional paradigms away from the laboratory. Our study further demonstrates the robustness of the oddball paradigm, providing an important step in understanding human cognition outside a controlled, laboratory setting. Additionally, the implementation of the e-skateboards (and e-scooters) offers a simple solution to the problem of motion artifacts during EEG data collection.

In other research, considerable efforts have been made to ensure that the contribution of motion artifact in the EEG data is managed effectively, such as the integration of portable EEG in experiments involving movement and action. For example, Makeig et al., (2009) developed the wearable mobile brain/body imaging (MOBI) to simultaneously record EEG, behavior and environmental events in order to get a richer set of data accounting for movements and interaction with the environment. Other studies involving data collection during movement (Gramman et al., 2010; Gwin et al,.2010) have shown that independent component analyses (ICAs) can be a practical solution to accounting for movement artifacts. Scanlon et al., (2017) compared the amount of single trial EEG noise between stationary pedaling and sitting and found that while cycling adds more noise to the data, an adequate enough amount of trials can yield

reliable ERP recordings. When it comes to cycling on the road, Scanlon et. al., (2017) found increases in trial noise during outside cycling in relation to a stationary, sitting condition. However, in terms of the P3 response, reliable recordings in obtained in all conditions, including during active outdoor cycling. Our e-skateboard paradigm greatly minimizes body movements while allowing for effective navigation, being greatly beneficial for the exploration of EEG responses in different moving environments.

Behavioral Results

In the current study, participants responded to target tones by pressing a button with their right hand. We calculated response accuracy and reaction time based on the four experimental conditions (preferred-clockwise, preferred-counter clockwise, non-preferred-clockwise, and non-preferred-counter clockwise) and by the grand averaged preferred and non-preferred conditions. We found no significant differences in accuracy or reaction time across conditions even though accuracy was marginally higher in the preferred stance condition. Additionally, there was larger standard deviation in the non-preferred condition for both accuracy and reaction time, suggesting that participants performed more uniformly in the preferred stance.

P3 & MMN/N2b Results

We hypothesized that the target-related P3 would be larger in the preferred stance condition due to differences in riding difficulty. Previous research shows that an increase in task difficulty (i.e., riding in one's least comfortable stance) should be reflected in a reduction of P3 amplitude (Kok, 2001; De Sanctic et al., 2014). However, we found no significant P3 differences between our conditions. Previous mobile EEG studies in naturalistic environments have shown a P3 amplitude decrease during naturalistic behaviors such as walking (Ladouce et al., 2019) and outdoor cycling (Zink et al., 2016; Scanlon et at., 2019; Scanlon et al., 2020). We expected that

the increase in difficulty in the non-preferred riding condition was going to be marked by a reduction in P3. However, we failed to find differences in our current paradigm. Considering that no behavioral differences in accuracy and reaction time were found by condition, it is possible that the change in stance preference did not interfere with the cognitive resources employed by the oddball task. Future paradigms should consider increasing the oddball task difficulty (e.g., manipulating tone frequency), or the non-preferred task difficulty (e.g. wobbly skateboards).

We also found a MMN/N2b difference between target-standard tones in all our experimental conditions. These results replicate previous EEG findings from other cycling studies in our research laboratory (Scanlon et al., 2017; Scanlon et al., 2019). This ERP component is elicited by sudden changes or deviations following the repeated presentation of a stimulus, such as the change from target to standard tones (Patel & Azzam, 2005). While the standard-target amplitude difference is present in all our conditions, we did not find differences in this component based on riding preference. The lack of differences in MMN/N2b amplitude is likely due to the environmental noise being the same in all task conditions for participants and this was reflected in similar ERP amplitude in all conditions.

Spectral Results

We recorded each participant's eyes open/close baseline spectra prior to completing the oddball task and found an expected significant increase in power within the alpha range (8-12 Hz) at electrodes Fz and Pz for the eyes-closed condition. Additionally, we found a complete attenuation of alpha power during the skateboard task relative to the baseline condition. These results support the findings of previous studies showing a decrease in alpha during complex behaviors such as walking (Beurskens et al., 2016; Storzer et al., 2016) and bicycle riding (Zink et al., 2016; Scanlon et al., 2020). Our current study serves as evidence that alpha is attenuated

while participant movement is being highly reduced by e-skateboarding. One of the exploratory goals of the present study was to assess whether riding preference influences pre-stimulus alpha power, based on our understanding that alpha power is modulated by increases in task demand (Foxe, et al., 2011). However, there were no significant differences in alpha power based on riding preference, while the overall desynchronization in alpha power we found is likely due to an overload of incoming stimuli from the task and environment (Klimesch et al., 2011). A second exploratory goal was to look at the influence of peripheral distractors in alpha lateralization. Depending on the riding orientation of the condition (clockwise or counterclockwise), distractors could systematically appear in either the right or left visual field of the subject for that block. Based on previous findings showing shifts in hemispheric alpha based on the location of spatial distractors (Sauseng et al., 2005; Kelly et al, 2006; Ikkai et al., 2016), we compared parieto-occipital alpha power across hemispheres but found no differences given riding orientation. This is likely due to the overall decrease in alpha power also observed in frontal and parietal central electrodes. We also looked at the overall left-right hemisphere alpha lateralization by riding preference. Studies have shown asymmetries based on handedness and footness (Packheiser et al., 2020), with skateboarding stance preference being tied to overall dominance based on anecdotal accounts from riders. We found no differences in overall lateralization based on riding preference.

A limitation of this study is that we failed to quantify the participants' perceived riding difficulty between the preferred and non-preferred conditions. This could have informed us about the degree of riding interference experienced by participants in the non-preferred condition and the relationship between subjective riding difficulty and overall ERP amplitude. Additionally, the oddball task used did not yield any behavioral differences between conditions. Given that the

field of mobile EEG is developing, obtaining behavioral effects in line with ERP results is an important step in understanding brain processes in real-life scenarios. Another was we did not measure torso muscle activity and acceleration on the body. Skateboarding has little overt movement, but relies on balance using the torso and proximal muscles of the legs and arms. Further research could correlate changes in these muscle groups during different riding conditions with brain activity and sensory input. Additionally, while this skateboard paradigm offers the opportunity to greatly minimize covert movements (in comparison to walking or bicycle riding paradigms), it does not eliminate muscle movements methodically. We wanted to test the influence of peripheral distractors (joggers and track users around the track) in terms of and alpha lateralization based on the notion that hemispheric alpha power is modulated by the location of distractors (Kelly et al, 2006), however, no spatial biasing manipulation was implemented (such as cueing participants into suppressing peripheral distractors). Future paradigms looking at peripheral distractors an alpha lateralization in mobile paradigms should systematically manipulate and quantify the location and degree of distractors relevant to the task in order to explore the role of alpha shifts in distractor suppression in real world environments.

Conclusion

The present study aimed to further understand EEG processes in real word environments using a novel skateboarding paradigm. We used a portable methodology developed in our laboratory and demonstrated that it is possible to obtain reliable EEG recordings while skateboarding in a complex scenario. While we found target-standard P3 and MMN/N2b differences in frontal and parietal regions, we found no differences in ERP amplitude based on riding difficulty. We also present evidence that the classic peak in resting state/eyes close alpha completely diminishes during eyes open and while skateboarding and this overall

desynchronization is the result of an increase load of incoming stimuli from the environment and task. The use of mobile EEG paradigms can open new avenues for the study of human cognition in naturalistic environments. As the field of mobile cognition grows, new paradigms can help us explore brain functioning in novel scenarios never accessible before. This new era of mobile cognition could have enormous potential in areas such as cognitive performance (driving, piloting, and error predictions), medicine and accessibility to data collection away from hospitals and laboratories, etc.

Acknowledgements

This research was supported by start-up funds from the faculty of science and an NSERC Discovery grant (#RES0024267) awarded to Kyle Elliot Mathewson. The authors would like you thank Pat Makhacheva for assistance in data collection, and Sarah Sheldon for analysis feedback.

Conflicts of Interest

No conflicts of interests have been declared by author(s).

Author contribution

Robles: design, data acquisition, analysis/interpretation, drafting

Kuziek: design, data acquisition, analysis/interpretation, drafting

Wlasitz: design, data acquisition, drafting

Bartlett: study conception, design, data acquisition

Hurd: study conception, design, critical revisions

Mathewson: design, analysis/interpretation, drafting, critical revisions

Data Accessibility Statement

This study's supporting data and analysis material is open to access using the following link: https://github.com/APPLabUofA/Skateboard

Abbreviations

ERP: Event Related Potential, EEG: Electroencephalography

References

Askamp, J., & van Putten, M. J. A. M. (2014) Mobile EEG in epilepsy. *Int. J. Psychophysiol.*, **91**, 30–35.

Caplan, J. B., Bottomley, M., Kang, P., & Dixon, R. A. (2015) Distinguishing rhythmic from non-rhythmic brain activity during rest in healthy neurocognitive aging. *NeuroImage*, **112**, 341–352.

Cruz-Garza, J. G., Brantley, J. A., Nakagome, S., Kontson, K., Megjhani, M., Robleto, D., & Contreras-Vidal, J. L. (2017) Deployment of mobile EEG technology in an art museum setting: Evaluation of signal quality and usability. *Front. Hum. Neurosci.*, **11**.

D'Atri, A., De Simoni, E., Gorgoni, M., Ferrara, M., Ferlazzo, F., Rossini, P. M., & De Gennaro, L. (2015) Frequency-dependent effects of oscillatory-tDCS on EEG oscillations: A study with better oscillation detection method (BOSC). *Arch. Ital. Biol.*, **153**, 2–3.

De Sanctis, P., Butler, J. S., Malcolm, B. R., & Foxe, J. J. (2014) Recalibration of inhibitory control systems during walking-related dual-task interference: A Mobile Brain-Body Imaging (MOBI) Study. *NeuroImage*, **94**, 55–64.

Delorme, A., & Makeig, S. (2004) EEGLAB: an open source toolbox for analysis of single-trial EEG dynamics including independent component analysis. *J. Neurosci. Methods*, **134**, 9–21.

Foxe, J. J., & Snyder, A. C. (2011) The role of alpha-band brain oscillations as a sensory suppression mechanism during selective attention. *Front. Psychol.*, **2**.

Gratton, G., Coles, M. G. ., & Donchin, E. (1983) A new method for off-line removal of ocular artifact. *Electroencephalogr. Clin. Neurophysiol.*, **55**, 468–484.

Gwin, J. T., Gramann, K., Makeig, S., & Ferris, D. P. (2010) Removal of movement artifact from high-density EEG recorded during walking and running. *J. Neurophysiol.*, **103**, 3526–3534.

Haller, M., Donoghue, T., Peterson, E., Varma, P., Sebastian, P., Gao, R., Noto, T., Knight, R. T., Shestyuk, A., & Voytek, B. (2018) Parameterizing neural power spectra. *BioRxiv*, 299859.

Hughes, A. M., Whitten, T. A., Caplan, J. B., & Dickson, C. T. (2012) BOSC: A better oscillation detection method, extracts both sustained and transient rhythms from rat hippocampal recordings. *Hippocampus*, **22**, 1417–1428.

Ikkai, A., Dandekar, S., & Curtis, C. E. (2016) Lateralization in Alpha-Band Oscillations Predicts the Locus and Spatial Distribution of Attention. *PLOS ONE*, **11**, e0154796.

Kelly, S. P., Gomez-Ramirez, M., & Foxe, J. J. (2009) The strength of anticipatory spatial biasing predicts target discrimination at attended locations: A high-density EEG study. *Eur. J. Neurosci.*, **30**, 2224–2234.

Kelly, S. P., Lalor, E. C., Reilly, R. B., & Foxe, J. J. (2006) Increases in alpha oscillatory power reflect an active retinotopic mechanism for distracter suppression during sustained visuospatial attention. *J. Neurophysiol.*, **95**, 3844–3851.

Klimesch, W., Doppelmayr, M., Russegger, H., Pachinger, T., & Schwaiger, J. (1998) Induced alpha band power changes in the human EEG and attention. *Neurosci. Lett.*, **244**, 73–76.

Kok, A. (2001) On the utility of P3 amplitude as a measure of processing capacity. *Psychophysiology*, **38**, 557–577.

Kontson, K. L., Megjhani, M., Brantley, J. A., Cruz-Garza, J. G., Nakagome, S., Robleto, D., White, M., Civillico, E., & Contreras-Vidal, J. L. (2015) Your brain on art: Emergent cortical dynamics during aesthetic experiences. *Front. Hum. Neurosci.*, **9**.

Kuziek, J. W. P., Redman, E. X., Splinter, G. D., & Mathewson, K. E. (2018) Increasing the mobility of EEG data collection using a Latte Panda computer. *J. Neurosci. Methods*, **308**, 34–47.

Ladouce, S., Donaldson, D. I., Dudchenko, P. A., & Ietswaart, M. (2019) Mobile EEG identifies the re-allocation of attention during real-world activity. *Sci. Rep.*, **9**.

Makeig, S., Gramann, K., Jung, T. P., Sejnowski, T. J., & Poizner, H. (2009) Linking brain, mind and behavior. *Int. J. Psychophysiol.*, **73**, 95–100.

Packheiser, J., Schmitz, J., Pan, Y., El Basbasse, Y., Friedrich, P., Güntürkün, O., & Ocklenburg, S. (2020) Using Mobile EEG to Investigate Alpha and Beta Asymmetries During Hand and Foot Use. *Front. Neurosci.*, **14**.

Patel, S. H., & Azzam, P. N. (2005) Characterization of N200 and P300: Selected studies of the Event-Related Potential. *Int. J. Med. Sci.*, **2**.

Picton, T. W. (1992) The P300 wave of the human event-related potential. *J. Clin. Neurophysiol.*, **9**, 456–479.

Puce, A., & Hämäläinen, M. S. (2017) A review of issues related to data acquisition and analysis in EEG/MEG studies. *Brain Sci.*, **7**.

Beurskens, R., Steinberg, F., Antonieeqicz, F., Wolff, W., & Granacher, U. (2016) Neural Correlates of Dual-Task Walking: Effects of Cognitive Versus Motor Interference in Young Adults. *Neural Plast.*, **2016**.

Sauseng, P., Klimesch, W., Stadler, W., Schabus, M., Doppelmayr, M., Hanslmayr, S., Gruber, W. R., & Birbaumer, N. (2005) A shift of visual spatial attention is selectively associated with human EEG alpha activity. *Eur. J. Neurosci.*, **22**, 2917–2926.

Scanlon, J. E. M., Redman, E. X., Kuziek, J. W. P., & Mathewson, K. E. (2020) A ride in the park: Cycling in different outdoor environments modulates the auditory evoked potentials. *Int. J. Psychophysiol.*, **151**, 59–69.

Scanlon, J. E. M., Sieben, A. J., Holyk, K. R., & Mathewson, K. E. (2017) Your brain on bikes: P3, MMN/N2b, and baseline noise while pedaling a stationary bike. *Psychophysiology*, **54**, 927–937.

Scanlon, J. E. M., Townsend, K. A., Cormier, D. L., Kuziek, J. W. P., & Mathewson, K. E. (2019) Taking off the training wheels: Measuring auditory P3 during outdoor cycling using an active wet EEG system. *Brain Res.*, **1716**, 50–61.

Sirevaag, E. J., Kramer, A. F., Wickens, C. D., Reisweber, M., Strayer, D. L., & Grenell, J. F. (1993) Assessment of pilot performance and mental workload in rotary wing aircraft. *Ergonomics*, **36**, 1121–1140.

Squires, N. K., Squires, K. C., & Hillyard, S. A. (1975) Two varieties of long-latency positive waves evoked by unpredictable auditory stimuli in man. *Electroencephalogr. Clin. Neurophysiol.*, **38**, 387–401.

Storzer, L., Butz, M., Hirschmann, J., Abbasi, O., Gratkowski, M., Saupe, D., Schnitzler, A., & Dalal, S. S. (2016) Bicycling and walking are associated with different cortical oscillatory dynamics. *Front. Hum. Neurosci.*, **10**.

Whitten, T. A., Hughes, A. M., Dickson, C. T., & Caplan, J. B. (2011) A better oscillation detection method robustly extracts EEG rhythms across brain state changes: The human alpha rhythm as a test case. *NeuroImage*, **54**, 860–874.

Zink, R., Hunyadi, B., Van Huffel, S., & De Vos, M. (2016) Mobile EEG on the Bike: Disentangling Attentional and Physical Contributions to Auditory Attention Tasks. *J. Neural Eng.*, **13**.